A novel design of fractional Mayer wavelet neural networks with application to the nonlinear singular fractional Lane-Emden systems

Zulqurnain Sabir[1], Muhammad Shoaib[2], Juan L.G. Guirao[3,*], Muhammad Asif Zahoor Raja[4]

[1,*]Department of Mathematics and Statistics, Hazara University, Mansehra, Pakistan
Email: zulqurnain_maths@hu.edu.pk

[2]Department of Mathematics, COMSATS University Islamabad, Attock Campus, Attock 43600, Pakistan
Email: dr.shoaib@cuiatk.edu.pk

[3]Department of Applied Mathematics and Statistics, Technical University of Cartagena, Hospital de Marina 30203-Cartagena, Spain
Email: juan.garcia@upct.es
* Corresponding author

[2]Department of Electrical and Computer Engineering, COMSATS University Islamabad, Attock Campus, Attock 43600, Pakistan
Email: muhammad.asif@ciit-attock.edu.pk

Abstract: In this study, a novel stochastic computational frameworks based on fractional Mayer wavelet artificial neural network (FMW-ANN) is presented for effective numerical treatment for nonlinear singular fractional Lane-Emden (NS-FLE) differential equation. The modeling strength of FMW-ANN is used to transformed the differential NS-FLE system to difference equations and approximate theory is implemented in mean squared error sense to develop a merit function for NS-FLE differential equations. Meta-heuristic strength of hybrid computing by exploiting global search efficacy of genetic algorithms (GA) supported with local refinements with efficient active-set (AS) algorithm is used for optimization of design variables FMW-ANN., i.e., FMW-ANN-GASA. The proposed FMW-ANN-GASA methodology is implemented on NS-FLM for six different scenarios in order to exam the accuracy, convergence, stability and robustness. The proposed numerical results of FMW-ANN-GASA are compared with exact solutions to verify the correctness, viability and efficacy. The statistical observations further validate the worth of FMW-ANN-GASA for the solution of singular nonlinear fractional order systems.

Keywords: Mayer wavelet kernels; Artificial neural networks; Genetic algorithms, active-set algorithm; hybrid-computing techniques; Lane-Emden equation; Singular Systems.

1. Introduction

The study of fractional differential equations (FDEs) is considered very important in almost all the field in-particular mathematics, physics, control systems and engineering. Fractional calculus and FDEs have been studied during the last three decades using different operators: few of paramount significance are Erdlyi-Kober operator [1], operator of the Riemann-Liouville [2], Caputo operator [3], Weyl-Riesz operator [4] and Grnwald-Letnikov operator [5]. The study of these fractional derivative operators has growing interest in the research community due to their use in the modeling of viscoplasticity [6-7], dynamic systems [8], thermal analysis of disk brakes [9], real materials [10], fluid mechanics [11], glass forming materials [12], electromagnetic theory [13], viscous dampers [14] and fast desorption process of methane in coal [15] and many more [16-17].

There are many linear/nonlinear, singular/nonsingular, initial, boundary value problems (BVPs) are considered very complicated to solve with traditional numerical and analytical procedure, one of such class is nonlinear singular Lane-Emden system. The Lane-Emden model exists in quantum mechanics as well as astrophysics and normally consider to be very stiff to be solved due to existence of singularity at the origin. Many deterministic techniques have been implemented to solve Lane-Emden equations such as homotopy perturbation technique [18], sinc-collocation technique [19], variational iteration technique [20] and many more [21-24] etc. All these analytical/numerical schemes have their own individual merits and drawbacks over one another, while stochastic numerical solver based on soft computing or machine learning methodologies have not be yet exploiting for the solution of nonlinear singular fractional Lane-Emden (NS-FLE) system. The general form of NS-FLE equation is given as [25]:

$$
\begin{aligned}
&D^{\alpha} y(x) + \frac{\lambda}{x^{\alpha-\beta}} D^{\beta} y(x) + f(x,y) = g(x), \\
&y(0) = c_0, \quad y(1) = d_0,
\end{aligned} \tag{1}
$$

where $0 < x \le 1,\ \lambda \ge 0,\ 0 < \alpha \le 2,\ 0 < \beta \le 1,\ c_0$ and d_0 are constants, $f(x,y)$ is a continuous function and D is fractional derivative operator. Aim of the present work is to solve the model (1) via intelligent computing techniques based on neural networks and their optimization with hybrid meta-heuristic methodologies.

The meta-heuristic based numerical computing has been extensively implemented by the research community for solving linear/nonlinear systems by functioning strength of neural networks (NN) and effective adaptation with evolutionary computing paradigms [26-30]. Some recent applications of the evolutionary computing are cell biology [31], nonlinear prey-predator models [32], nonlinear reactive transport model [33], nonlinear Troesch's problem [34], nonlinear singular Thomas-Fermi systems [35], nonlinear doubly singular systems [36], micropolar fluid flow [37], magnetohydrodynamic flow [38], heartbeat model [39], control systems [40], heat conduction model of the human head [41], power [42] and energy [43]. These contributions have been proven the value, worth and significance of stochastic solvers based on convergence, accuracy and robustness.

Keeping in view all these application, authors are interested to explore/exploit the stochastic numerical solvers for, reliable, efficient and stable technique for solving the NS-FLE equation. Aim of the present work is to solve the model (1) via intelligent computing based on fractional Mayer wavelet artificial neural network (FM-ANN) optimized by the hybrid strength of genetic algorithm (GA) and active-set (AS) algorithm, i.e., FMM-ANN-GAAS. The salient features of proposed FMM-ANN-GAAS are listed as follows:

- Novel design of fractional Mayer wavelet neural network optimized with integrated heuristics of GA aided with AS algorithm is presented for solving variants of fractional Lane-Emden system represented with singular nonlinear differential equations involving fractional derivative terms.
- The proposed FMM-ANN-GAAS scheme is applied for variants of NS-FLE systems and comparison of the results from available exact solution verify the correctness for solving these singular fractional order systems.
- The performance accreditation established through results of statistical investigations in terms of semi interquartile range, mean absolute error, Theil's inequality coefficient and root mean square error measures.
- The simple coherent structure of Mayer wavenets, availability of solutions on entire continuous training domain, smooth implementation procedure, reliable, robust, stability, extendibility are other worry assurances of the proposed stochastic numerical solver.

Remaining of the paper is organized as follows. In section 2, the design procedure adopted for formulation of Mayer wavenet and their optimizations with hybrid computation heuristics of GAAS algorithm. In Section 3, an overview of the performance indices is presented. In Section 4, numerical experimentations of proposed FM-ANN-GAAS is presented along with the observations on statistics. In Section 5, the concluding remarks and future research opening are listed.

2. Designed Methodology

The FMW-ANN is designed for solving singular FDEs in this section. The formulation for designing the differential equation models, fitness function, and optimization procedure based on combination of GA-ASA is presented here.

2.1 Fractional Mayer Wavelet Neural Network

The ANN based models are familiar to provide the solution for the number of applications in various fields [44-45]. In the FMW-ANN; $\hat{y}(x)$ is used for the proposed solution and its n^{th} order integer derivatives is $D^{(n)}\hat{y}(x)$ while the fractional order derivative is $D^{\alpha}\hat{y}(x)$, and expression of these networks are respectively given as:

$$\hat{y}(x) = \sum_{i=1}^{m} a_i f(b_i x + c_i)$$

$$D^{(n)} \hat{y}(x) = \sum_{i=1}^{m} a_i D^{(n)} f(b_i x + c_i) \tag{2}$$

$$D^{\alpha} \hat{y}(x) = \sum_{i=1}^{m} a_i D^{\alpha} f(b_i x + c_i)$$

where *m* represents the number of neurons, ***a***, ***b*** and ***c*** are the vector component of weight matrix ***W*** as:

$\boldsymbol{W} = [\boldsymbol{a}, \boldsymbol{b}, \boldsymbol{c}]$, for $\boldsymbol{a} = [a_1, a_2, ..., a_m], \boldsymbol{b} = [b_1, b_2, ..., b_m]$ and $\boldsymbol{c} = [c_1, c_2, ..., c_m]$

while, the Mayer wavelet kernel is defined as:

$$f(x) = 35x^4 - 84x^5 + 70x^6 - 20x^7 \tag{3}$$

Using the Mayer wavelet kernel in the equation (3) in set of equations (2), we have:

$$\hat{y}(x) = \sum_{i=1}^{m} a_i \left(35(b_i x + c_i)^4 - 84(b_i x + c_i)^5 + 70(b_i x + c_i)^6 - 20(b_i x + c_i)^7\right),$$

$$D^{(n)} \hat{y}(x) = \sum_{i=1}^{m} a_i \begin{pmatrix} 35D^{(n)}(b_i x + c_i)^4 - 84D^{(n)}(b_i x + c_i)^5 + 70D^{(n)}(b_i x + c_i)^6 \\ -20D^{(n)}(b_i x + c_i)^7 \end{pmatrix}, \tag{4}$$

$$D^{\alpha} \hat{y}(x) = \sum_{i=1}^{m} a_i \begin{pmatrix} 35D^{\alpha}(b_i x + c_i)^4 - 84D^{\alpha}(b_i x + c_i)^5 + 70D^{\alpha}(b_i x + c_i)^6 \\ -20D^{\alpha}(b_i x + c_i)^7 \end{pmatrix},$$

The arbitrary combination of the FMW-ANN can be used to solve NS-FLE system (1) subject to availability of appropriate weight matrix *W*. In order to determine the weights of FMW-ANN, one may exploit the approximation theory in mean squared error sense to formulate a fitness function *E* as:

$$E = E_1 + E_2, \tag{5}$$

where E_1 is the error function related to NS-FLE equation (1) and E_2 is used for initial conditions for the model (1), and are respectively given as:

$$E_1 = \frac{1}{N} \sum_{i=1}^{m} \left(D^{\alpha} \hat{y}_m + \frac{\lambda}{x_m^{\alpha-\beta}} D^{\beta} \hat{y}_m + f(x_m, y_m) - g_m \right)^2, \tag{6}$$

$$E_2 = \frac{1}{2}\left((\hat{y}_0 - A)^2 + (\hat{y}_N - B)^2\right), \tag{7}$$

for $N = \frac{1}{h},\ \hat{y}_m = \hat{y}(x_m),\ g_m = g(x_m) x_m = mh$.

One may determine the solution of NS-FLE model (1) with the obtainability of suitable weights ***W***, such that $E \to 0$, the approximate outcomes of FMW-ANN become neat to identical with the exact/optimal solutions, *i.e.,* $[\hat{y} \to y]$.

2.2 Networks optimization

The optimization of parameter for FMW-ANN is carried out using the hybrid computing framework based on GAs and AS techniques.

Genetic Algorithm is an optimization solver for the constrained/unconstrained global optimization problems and formulated on mathematical modelling of natural genetic process. GAs continually changes a population of individual, i.e., candidate solutions of optimization task and has ability to solve a variety of optimization problems by incorporated its reproduction tools via crossover, selection, elitism and mutation operators. Recently applications address with GAs include optimization of steel space frames with semi-rigid connections [46], control structure for a car-like robot [47], modelling and identification of nonlinear multivariable systems [48], optimization of investments in Forex markets with high leverage [49], a fully customizable hardware implementation [50], characterization of hyperelastic materials [51], evaluation of apparent shear stress in prismatic compound channels [52], detection of loss of coolant accidents of nuclear power plants [53], torque estimation problem [54] and prediction of biosorption capacity [55]. GAs hybridized with local search technique can upgrade its laziness trough the optimization procedure.

Active-set algorithm is an efficient local search methodology for rapid fine tuning of optimization tasks in different applications arising in broad fields. AS method belongs to efficient convex optimization solver exploit for both constrained and unconstrained problems. Few renewed applications addressed effectively by AS algorithm are models of Sisko fluid flow and heat transfer [56], for optimization extreme learning machines [57], symmetric eigenvalue complementarity problem [58], induction motor models [59], sidescan sonar image segmentation [60] and cardiac defibrillation [61].

The hybridization of GAs with AS, i.e., GAAS, is exploited for finding the design variables of FMW-ANN in order to solve the NS-FLE system. The brief descriptive procedure of optimization with GAAS algorithm in the form of pseudocode is presented in Table 1.

Table 1: Pseudo code of GAAS optimization tool to find the weights of FMW-ANN

```
Genetic Algorithms started
      Inputs:
            The chromosome with entries equal to weights of FMW-ANN as:
```
$W = [a, b, c]$ for $a = [a_1, a_2, ..., a_m], b = [b_1, b_2, ..., b_m]$, and $c = [c_1, c_2, ..., c_m]$
```
            Initial population based on n number of chromosome's W as:
```
$P = [W_1, W_2, ,..., W_n]^t$, for $w_i = [a_i, b_i, ..., c_i]^t$
```
      Output:
            The best optimized weights for FMW-ANN by GA, W_Best-GA.
      Initialization
            Construct W with real bounded entries and set of W to form P.
Set         settings of 'GA' and 'gaoptimset' routines
      Fitness evaluation
            Obtained the E for each W in P by equations (5).
      Termination
            Terminate the for any of the following
            'Fitness'' E → 10^-15, Tolerances 'TolFun'→10^-20, 'TolCon'→10^-20,
            'StallGenLimit' →100. 'Generations'→75, 'PopulationSize'→ 300
            and default other.
            Go to step storage, when termination condition meets,
      Ranking
            Ranked each W of P on E given in equation (5).
      Reproduction
            Create new P using Selection, Crossover and Mutations routines
            '@selectionuniform','@crossoverheuristic' and
            '@mutationadaptfeasible', respectively. Four best ranked W of P
            for elitism:
            Go to 'fitness evaluation' step
      Storage
            Save W_Best-GA, E, with time, generation and function counts.
End Genetic algorithms
AS procedure Started
      Inputs
            The initial weights of GA, W_Best-GA
      Output
            The best weights for FMW-ANN by GAAS method, W_GAAS
      Initialize
            Initial weights of GAs, W_Best-GA, as a start point of the algorithm
            Set bounded, constraints limits, iterations and other
      Terminate
            Stop in case of
            'Fitness' E ≤ 10^-14, 'iterations'' = 700, tolerances 'TolFun' ≤
            10^-20, 'TolX' ≤ 10^-20, ''TolCon'' ≤ 10^-20, 'MaxFunEvals' ≤ 200000
and         default others
      While (Terminate conditions attained)
            Fitness calculation
                  Determined the fitness E by equations (5.
            Fine Tuning
                  Use 'fmincon' routine with algorithm 'active-set' for
rapid                   modification of W at each cycle.
                  Go to fitness calculation step with improved W
      End While loop
      Accumulate
            Store the W_GAAS, E, time, iterations and function counts.
ASA Procedure End
```

3. Performance indices

The performance measures, used to analyzing strength and weaknesses of proposed FMW-ANN-GASA methodology for solving the variants of NS-FLM system, incorporated in this study are Theil's inequality coefficient (TIC), mean absolute deviation (MAD) and root mean square error (RMSE) as well as their average gauges named as Global TIC (G-TIC), Global MAD (G-MAD), and Global RMSE (G-RMSE). The definitions of TIC, MAD and RMSE in terms of the exact solution y and approximate solution $\hat{y}$ are given, respectively, as:

$$\text{TIC}=\frac{\sqrt{\frac{1}{n}\sum_{m=1}^{n}\left(y_m-\hat{y}_m\right)^2}}{\left(\sqrt{\frac{1}{n}\sum_{m=1}^{n}y_m^2}+\sqrt{\frac{1}{n}\sum_{m=1}^{n}\hat{y}_m^2}\right)}, \tag{8}$$

$$\text{MAD}=\sum_{m=1}^{n}\left|y_m-\hat{y}_m\right|, \tag{9}$$

$$RMSE=\sqrt{\frac{1}{n}\sum_{m=1}^{n}\left(y_m-\hat{y}_m\right)^2}, \tag{10}$$

where n represents the number of grid points. The optimal values of TIC, MAD and RMSE metrics are zeros in case of perfect modelling. The average values of The definitions of TIC, MAD and RMSE measures on the basis of sufficient large number of trials represents G-TIC, G-MAD), and G-RMSE, respectively. The optimal values of TIC, MAD and RMSE metrics as well as their global variant are zeros in case of perfect modelling.

4. Simulation and Results

The results of detailed simulations for FMW-ANN-GAAS for solving NS-FLE equation is presented here for six different cases in order to evaluate the performance. The results of FMW-ANN-GAAS on single and multiple trails for all the six cases of NS-FLE model are plotted with enough graphical and numerical illustrations to evaluate the accuracy and convergence.

Problem I:

Consider the NS-FLE differential equation (1) based system after multiplication denominator of second term both sides and homogeneous boundary condition by taking $c_o = d_0 = 0$ as:

$$\begin{aligned} &x^{\alpha-\beta}D^{\alpha}y(x)+\lambda D^{\alpha}y(x)+x^{\alpha-\beta}f(x,y)=x^{\alpha-\beta}g(x),\\ &y(0)=0,\ y(1)=0, \end{aligned} \tag{11}$$

By substituting $l=\alpha-\beta$, $h(x,y)=x^{\alpha-\beta}f(x,y)$ and $j(x)=x^{\alpha-\beta}g(x)$, we have

$$x^l D^\alpha y(x) + \lambda D^\alpha y(x) + h(x,y) = j(x),$$
$$y(0)=0,\ y(1)=0, \tag{12}$$

The particular expressions used for functions $h(x,y)$ and $j(x)$ as:

$$h(x,y) = x^{2-\alpha} y(x),$$
$$j(x) = (\lambda + x^l)\left(\frac{\Gamma(p+1)}{\Gamma(p-\alpha+1)} x^{p-\alpha} - \frac{\Gamma(q+1)}{\Gamma(q-\alpha+1)} x^{q-\alpha}\right) + x^{p+\alpha} - x^{q+\alpha}, \tag{13}$$

for positive integers p and q.

Using the relation in (13) in equation (12), we have

$$x^l D^\alpha y(x) + \lambda D^\alpha y(x) + \frac{1}{x^{\alpha-2}} y(x) = (\lambda + x^l)\left(\frac{\Gamma(p+1)}{\Gamma(p-\alpha+1)} x^{p-\alpha} - \frac{\Gamma(q+1)}{\Gamma(q-\alpha+1)} x^{q-\alpha}\right) + x^{p-\alpha+2} - x^{q-\alpha+2},$$
$$y(0)=0,\ y(1)=0, \tag{14}$$

The exact solution of the NS-FLE equation (14) is written as:

$$y(x) = x^p - x^q \tag{15}$$

Now for particular values of p = 3 and q = 4, NS-FLE equation (14) and its solution (15) are given as

$$x^l D^\alpha y(x) + \lambda D^\alpha y(x) + \frac{1}{x^{\alpha-2}} y(x) = (\lambda + x^l)\left(\frac{6}{\Gamma(4-\alpha)} x^{3-\alpha} - \frac{2}{\Gamma(q-\alpha+1)} x^{2-\alpha}\right) + x^{5=\alpha} - x^{4-\alpha},$$
$$y(0)=0,\ y(1)=0, \tag{16}$$
$$y(x) = x^3 - x^2$$

The error based fitness function of equation (16) using equation (5) is given as:

$$E = \frac{1}{N}\sum_{i=1}^{m}\left(\begin{array}{l} x_m^l D^\alpha \hat{y}_m + \lambda D^\alpha \hat{y}_m + \frac{1}{x_m^{\alpha-2}} - x_m^{5-\alpha} + x_m^{4-\alpha} \\ -\left(\lambda + x_m^l\right)\left(\frac{6}{\Gamma(4-\alpha)} x_m^{3-\alpha} - \frac{2}{\Gamma(q-\alpha+1)} x_m^{2-\alpha}\right) \end{array}\right)^2 + \frac{1}{2}\left(\left(\hat{y}_0\right)^2 + \left(\hat{y}_m\right)^2\right) \tag{17}$$

Six cases of NS-FLE system (11) are considered by taking different values of α, l and λ as listed in Table 2.

Optimization variables of FMW-ANN, to analyze all six variants of NS-FLE system (16), is conducted with the combination of global and local search strength of GAAS as per procedure listed in pseudocode given in Table 1. The whole procedure listed in Table 1 is repeated for hundred number of runs to create a large dataset of FMW-ANN parameters. These trained weights of FMW-ANN are used in first equation of set (4) to calculate the approximate solution for each case of the NS-FLE equation. The mathematical expressions derived by one set of optimized parameters, as shown in Figure 1, of FMW-ANN by GAAS technique for each case of NS-FLE system are given as:

$$\begin{aligned}\hat{y}_{C-1} &= 0.3092\left(35(0.5439x-0.0916)^4-84(0.5439x-0.0916)^5+70(0.5439x-0.0916)^6-20(0.5439x-0.0916)^7\right)\\ &\quad -0.4219\left(35(0.0499x-0.0930)^4-84(0.0499x-0.0930)^5+70(0.0499x-0.0930)^6-20(0.0499x-0.0930)^7\right)\\ &\quad +\ldots+1.0940\left(35(0.2980x-0.1071)^4-84(0.2980x-0.1071)^5+70(0.2980x-0.1071)^6-20(0.2980x-0.1071)^7\right),\end{aligned} \tag{18}$$

$$\begin{aligned}\hat{y}_{C-2} &= 0.7889\left(35(0.5916x+0.7570)^4-84(0.5916x+0.7570)^5+70(0.5916x+0.7570)^6-20(0.5916x+0.7570)^7\right)\\ &\quad +0.3089\left(35(-0.6838x+0.2450)^4-84(-0.6838x+0.2450)^5+70(-0.6838x+0.2450)^6-20(-0.6838x+0.2450)^7\right)\\ &\quad +\ldots-0.9791\left(35(0.0210x+0.8873)^4-84(0.0210x+0.8873)^5+70(0.0210x+0.8873)^6-20(0.0210x+0.8873)^7\right),\end{aligned} \tag{19}$$

$$\begin{aligned}\hat{y}_{C-3} &= 1.5378\left(35(1.1811x-0.0566)^4-84(1.1811x-0.0566)^5+70(1.1811x-0.0566)^6-20(1.1811x-0.0566)^7\right)\\ &\quad -0.3133\left(35(-1.3617x+2.0217)^4-84(-1.3617x+2.0217)^5+70(-1.3617x+2.0217)^6-20(-1.3617x+2.0217)^7\right)\\ &\quad +\ldots+0.2656\left(35(-0.5513x+1.7973)^4-84(-0.5513x+1.7973)^5+70(-0.5513x+1.7973)^6-20(-0.5513x+1.7973)^7\right),\end{aligned} \tag{20}$$

$$\begin{aligned}\hat{y}_{C-4} &= -0.1797\left(35(-0.0208x-0.09161)^4-84(-0.0208x-0.09161)^5+70(-0.0208x-0.09161)^6-20(-0.0208x-0.09161)^7\right)\\ &\quad +2.5514\left(35(-0.0415x-0.1137)^4-84(-0.0415x-0.1137)^5+70(-0.0415x-0.1137)^6-20(-0.0415x-0.1137)^7\right)\\ &\quad +\ldots-1.4951\left(35(-0.1646x+0.1344)^4-84(-0.1646x+0.1344)^5+70(-0.1646x+0.1344)^6-20(-0.1646x+0.1344)^7\right),\end{aligned} \tag{21}$$

$$\begin{aligned}\hat{y}_{C-5} &= -8.0125\left(35(0.5327x+0.4259)^4-84(0.5327x+0.4259)^5+70(0.5327x+0.4259)^6-20(0.5327x+0.4259)^7\right)\\ &\quad +1.1136\left(35(-0.5186x-0.5861)^4-84(-0.5186x-0.5861)^5+70(-0.5186x-0.5861)^6-20(-0.5186x-0.5861)^7\right)\\ &\quad +\ldots-0.6563\left(35(1.0788x+1.2783)^4-84(1.0788x+1.2783)^5+70(1.0788x+1.2783)^6-20(1.0788x+1.2783)^7\right),\end{aligned} \tag{22}$$

$$\begin{aligned}\hat{y}_{C-6} &= 0.2908\left(35(0.3358x-0.9622)^4-84(0.3358x-0.9622)^5+70(0.3358x-0.9622)^6-20(0.3358x-0.9622)^7\right)\\ &\quad +0.0007\left(35(0.2163x-1.0749)^4-84(0.2163x-1.0749)^5+70(0.2163x-1.0749)^6-20(0.2163x-1.0749)^7\right)\\ &\quad +\ldots+1.4015\left(35(-0.1081x-0.4119)^4-84(-0.1081x-0.4119)^5+70(-0.1081x-0.4119)^6-20(-0.1081x-0.4119)^7\right),\end{aligned} \tag{23}$$

Table 2: Variants of NS-FLE system

Index	Parametric values		
	α	l	λ
Case-1	1.2	0.7	1
Case-2	1.5	1	1
Case-3	1.8	1.3	1
Case-4	1.2	0.7	3
Case-5	1.5	1	3
Case-6	1.8	1.3	3

The approximate solutions $\hat{y}(x)$ are determined by equations. (18-23) and outcomes are graphically illustrated in Figure 2 and numerically in Table 3 along with reference exact solution for each case of NS-FLE equation (16). The exact and proposed results of FMW-ANN-GAAS overlap for all six cases of NS-FLE equation. To analyse the matching order of the results, the absolute error (AE) from exact solutions are calculated for all six cases NS-FLE equation and outcomes are plotted in Figure 2 and tabulated in Table 4. To performance indices of TIC, MAD, RMSE and fitness as indicated in equations (8), (9), (10) and (17) are calculated and result are provided graphically in Figure 3 for each case. All these illustrations evidently show that FMW-ANN-GAAS solutions are in a good agreement with the reference exact solutions in all six cases of NS-FLE equation. Near optimum values are obtained for each the performance metric that further established the worth of the proposed FMW-ANN-GAAS scheme.

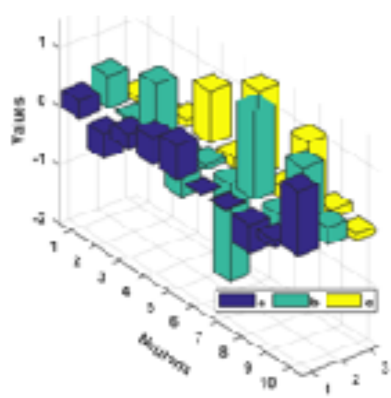

(a):weights for Case 1

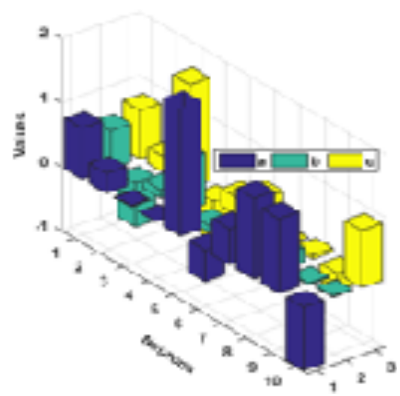

(b):weights for Case 2

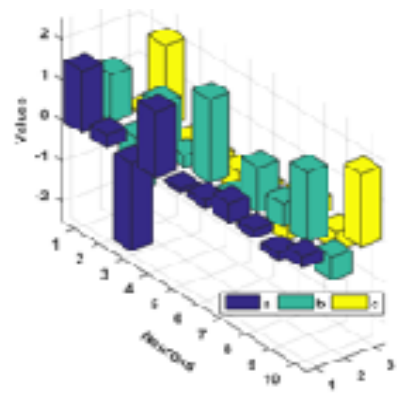

(c):weights for Case 3

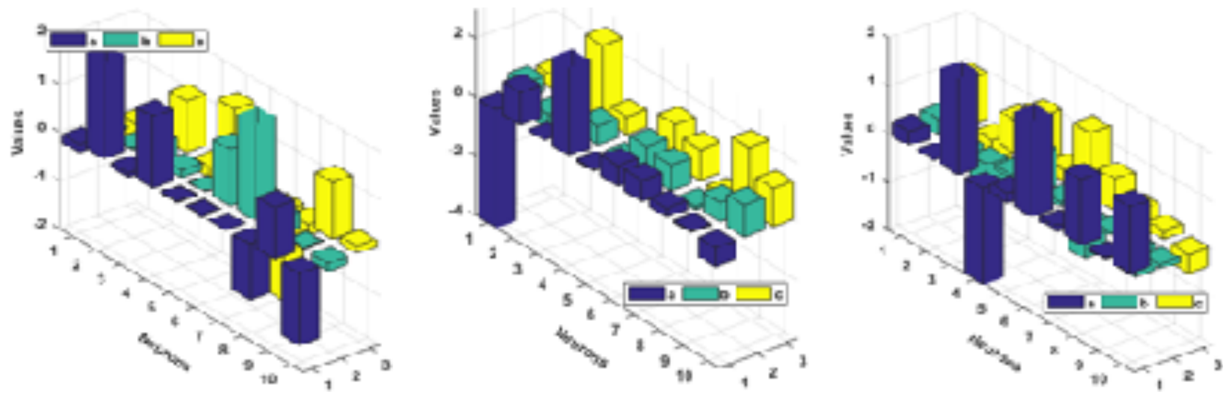

(d):weights for Case 4 **(e):weights for Case 5** **(f):weights for Case 6**

Figure 1: Set of trained weight vectors of FMW-ANN for cases 1 to 6 of NS-FLE system

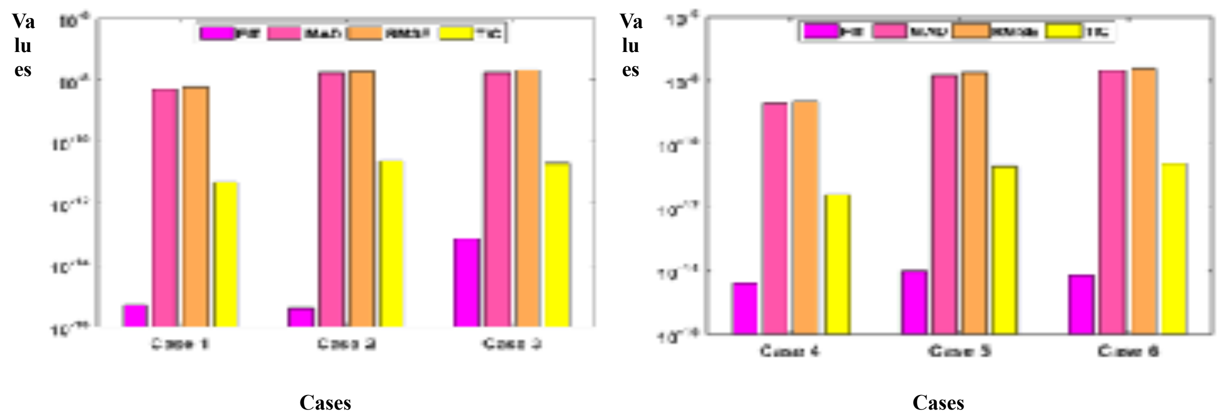

(a) NS-FLE equation for Cases 1-3 (b) NS-FLE equation for Cases 4-6

Figure 3: The magnitude of performance indices for each case of NS-FLE system

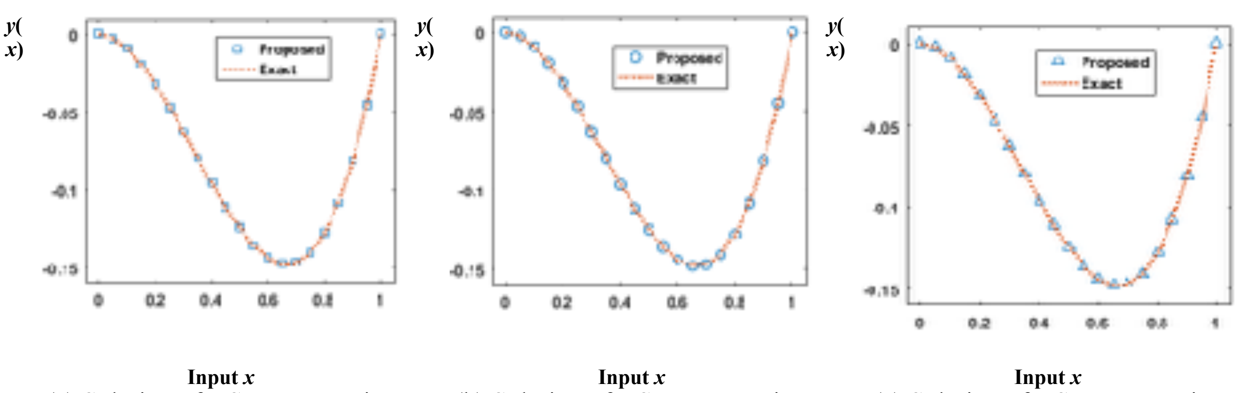

(a) Solution of NS-FLE equation Case 1 (b) Solution of NS-FLE equation Case 2 (c) Solution of NS-FLE equation Case 3

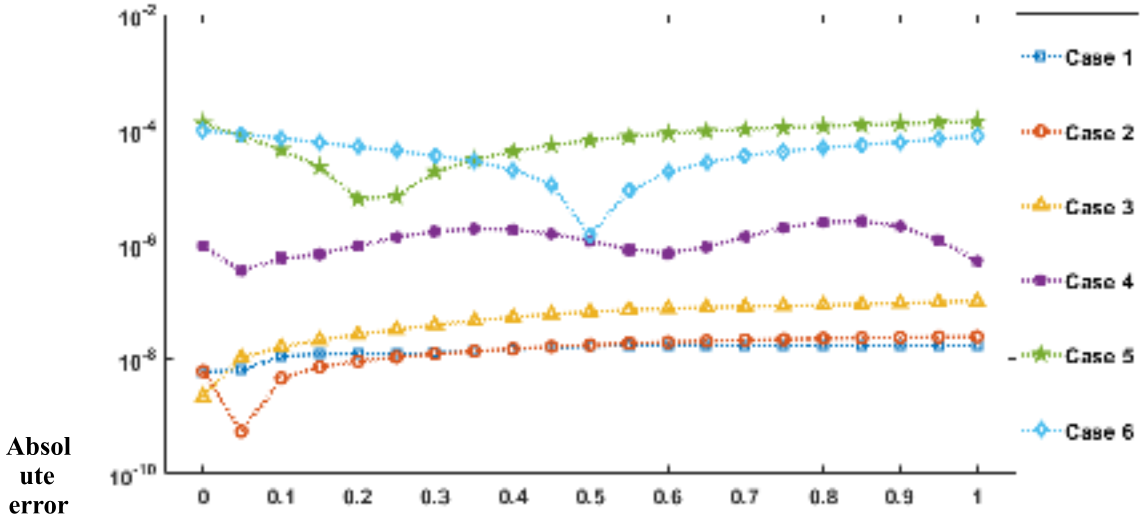

Input *x*
(g) Absulte error from exact solution for NS-FLE equation

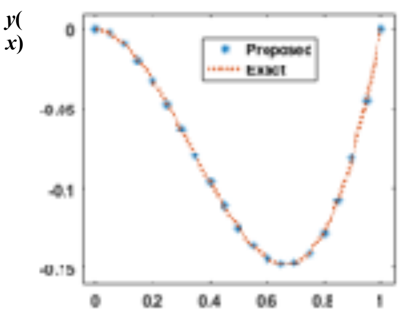

Input *x*
(a) Solution of NS-FLE equation Case 4

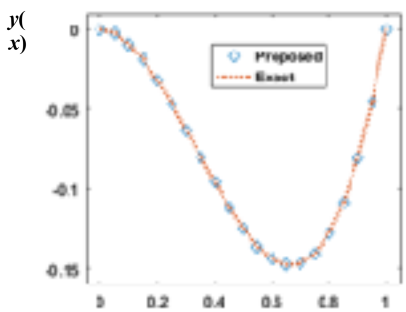

Input *x*
(b) Solution of NS-FLE equation Case 5

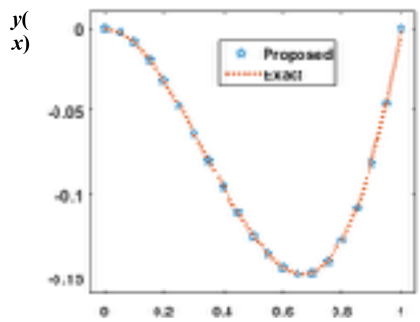

Input *x*
(c) Solution of NS-FLE equation Case 6

Figure 2: Comparison of results of FMW-ANN-GAAS from exact solution for all six case of the NS-FLE system

Table 3: Results of FMW-ANN-GAAS and exact solution for each variant of NS-FLE system

x	**Exact Solution** $y(x)$	**Approximate Solution** $\hat{y}(x)$					
		Case-1	**Case-2**	**Case-3**	**Case-4**	**Case-5**	**Case-6**
0	0.000000000	-0.000000009	-0.000000006	0.000000066	-0.000000002	-0.000000055	-0.000000051

0.05	-0.002375000	-0.002374999	-0.002374999	-0.002374946	-0.002375001	-0.002375040	-0.002375047
0.1	-0.009000000	-0.008999992	-0.008999995	-0.008999962	-0.009000000	-0.009000031	-0.009000043
0.15	-0.019125000	-0.019124988	-0.019124993	-0.019124978	-0.019125000	-0.019125025	-0.019125040
0.2	-0.032000000	-0.031999988	-0.031999991	-0.031999990	-0.032000000	-0.032000020	-0.032000037
0.25	-0.046875000	-0.046874991	-0.046874989	-0.046874998	-0.046875000	-0.046875016	-0.046875034
0.3	-0.063000000	-0.062999994	-0.062999988	-0.063000003	-0.062999999	-0.063000013	-0.063000031
0.35	-0.079625000	-0.079624996	-0.079624987	-0.079625005	-0.079624999	-0.079625009	-0.079625028
0.4	-0.096000000	-0.095999997	-0.095999985	-0.096000006	-0.095999998	-0.096000005	-0.096000026
0.45	-0.111375000	-0.111374997	-0.111374984	-0.111375008	-0.111374998	-0.111375001	-0.111375023
0.5	-0.125000000	-0.124999995	-0.124999983	-0.125000009	-0.124999998	-0.124999998	-0.125000021
0.55	-0.136125000	-0.136124994	-0.136124982	-0.136125011	-0.136124999	-0.136124995	-0.136125018
0.6	-0.144000000	-0.143999992	-0.143999981	-0.144000014	-0.143999998	-0.143999992	-0.144000016
0.65	-0.147875000	-0.147874992	-0.147874980	-0.147875016	-0.147874998	-0.147874990	-0.147875013
0.7	-0.147000000	-0.146999994	-0.146999979	-0.147000018	-0.146999997	-0.146999988	-0.147000011
0.75	-0.140625000	-0.140624996	-0.140624978	-0.140625020	-0.140624996	-0.140624986	-0.140625008
0.8	-0.128000000	-0.127999999	-0.127999978	-0.128000021	-0.127999996	-0.127999984	-0.128000006
0.85	-0.108375000	-0.108375001	-0.108374977	-0.108375023	-0.108374996	-0.108374981	-0.108375003
0.9	-0.081000000	-0.081000002	-0.080999977	-0.081000026	-0.080999996	-0.080999979	-0.081000001
0.95	-0.045125000	-0.045125000	-0.045124976	-0.045125029	-0.045124998	-0.045124976	-0.045124999
1	0.000000000	0.000000002	0.000000024	-0.000000034	0.000000001	0.000000026	0.000000003

Table 4: Comparison of FMW-ANN-GAAS results on the basis of absolute error form exact solutions for each case of NS-FLE system

x	Absolute Error $\lvert y(x) - \hat{y}(x) \rvert$					
	Case-1	**Case-2**	**Case-3**	**Case-4**	**Case-5**	**Case-6**
0	8.817E-09	6.010E-09	6.581E-08	1.829E-09	5.512E-08	5.136E-08
0.05	8.001E-10	5.541E-10	5.427E-08	5.155E-10	4.041E-08	4.677E-08
0.1	8.187E-09	4.536E-09	3.766E-08	4.287E-10	3.119E-08	4.315E-08
0.15	1.167E-08	7.101E-09	2.204E-08	4.212E-10	2.503E-08	3.999E-08
0.2	1.161E-08	8.966E-09	1.001E-08	1.200E-10	2.039E-08	3.701E-08
0.25	9.356E-09	1.054E-08	2.051E-09	4.334E-10	1.637E-08	3.412E-08
0.3	6.429E-09	1.201E-08	2.546E-09	1.038E-09	1.253E-08	3.127E-08
0.35	4.077E-09	1.344E-08	4.948E-09	1.496E-09	8.721E-09	2.848E-08
0.4	3.012E-09	1.484E-08	6.320E-09	1.703E-09	4.966E-09	2.576E-08
0.45	3.354E-09	1.616E-08	7.549E-09	1.674E-09	1.369E-09	2.314E-08
0.5	4.714E-09	1.737E-08	9.127E-09	1.529E-09	1.956E-09	2.059E-08
0.55	6.384E-09	1.847E-08	1.117E-08	1.441E-09	4.935E-09	1.810E-08
0.6	7.569E-09	1.944E-08	1.350E-08	1.574E-09	7.555E-09	1.563E-08
0.65	7.637E-09	2.030E-08	1.583E-08	2.018E-09	9.868E-09	1.317E-08
0.7	6.328E-09	2.107E-08	1.789E-08	2.741E-09	1.199E-08	1.070E-08
0.75	3.882E-09	2.176E-08	1.959E-08	3.567E-09	1.406E-08	8.231E-09
0.8	1.038E-09	2.240E-08	2.111E-08	4.198E-09	1.623E-08	5.795E-09
0.85	1.139E-09	2.297E-08	2.290E-08	4.301E-09	1.859E-08	3.434E-09
0.9	1.649E-09	2.348E-08	2.552E-08	3.661E-09	2.116E-08	1.184E-09
0.95	2.096E-10	2.391E-08	2.935E-08	2.429E-09	2.381E-08	9.623E-10
1	1.777E-09	2.429E-08	3.409E-08	1.477E-09	2.620E-08	3.110E-09

The analysis of the performance of FMW-ANN-GAAS to solve NS-FLE system (16) is conducted through statistics and results are presented in figures 4 to 9 and tables 5 to 10 for 100 independent executions.

Statistical results by means of minimum (Min), Maximum (Max), median (Med), and semi interquartile range (SIR), i.e., SIR is basically one half of the difference of 3rdquartile (Q_3=75% data) and 1stquartile (Q_1=25% data), are calculated for 100 executions of FMW-ANN-GAAS to solve all six cases of NS-FLE equation (16). These statistical observations are used for precision analysis of presented FMW-ANN-GAAS technique. The independent execution of the algorithm with parameter of FWM-ANN attaining the MIN and MAX error based fitness value is called the best and worst run, respectively. The results of NS-FLE equation for the best, mean and exact solution are plotted in Figure 4, while the values of AE for the best, worst and mean are tabulated in Figure 5. The best AE values lie between the ranges of 10^{-07} to 10^{-10}, while, the reasonably accuracy of mean values for each case of the NS-FLE equation. The statistics by means of Min, Max, Med and SIR operator are tabulated in tables 5, 6 and 7 for cases (1-2), (3-4) and (5-6) of NS-FLE equation (16), respectively. It is clear that the scale of Min values lies around 10^{-08} to 10^{-09} which Max values also lies in good ranges for each case of NS-FLE model. Similarly, the median values also showed good results and lie around 10^{-04} to 10^{-05}. Finally, the SIR values lie around 10^{-03} to 10^{-05} that indicates very good ranges for each case of NS-FLE model.

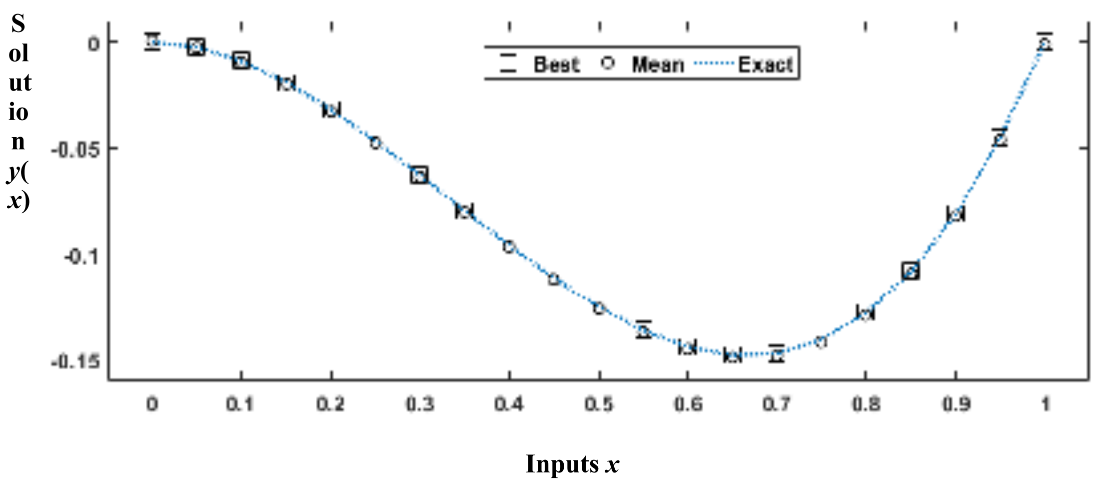

Figure 4: Statistical operators based comparison of results through exact solutions for case 1 of NS-FLE system

The result of statistics in terms of fitness, MAD, RMSE and TIC gauges are plotted in figures 6, 7, 8 and 9, respectively for all six cases of NS-FLE equation (16). The histograms illustrations are used to find the tendency or trend of the results of fitness, MAD, RMSE and TIC, and are also provided for in figures 6 to 9, respectively. One may clearly understand that over 80% of independent implementations of FMW-ANN-GAAS obtained very good fitness, MAD, RMSE and TIC gauges for each case of NS-FLE system. All these results represent that over 80% of the runs of FMW-ANN-GAAS attained precise values of each performance measures.

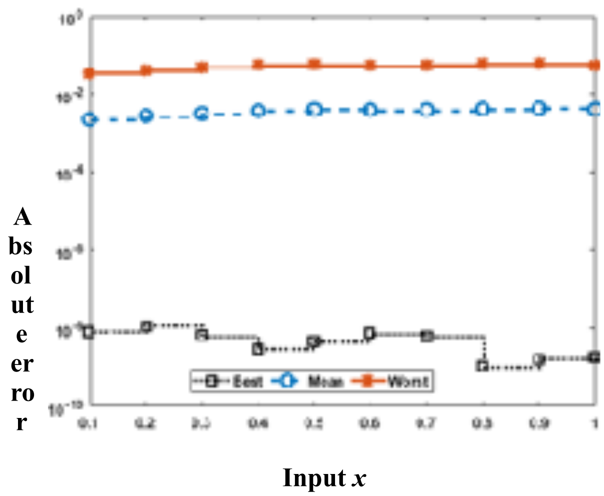

(a) Results of NS-FLE equation Case 1

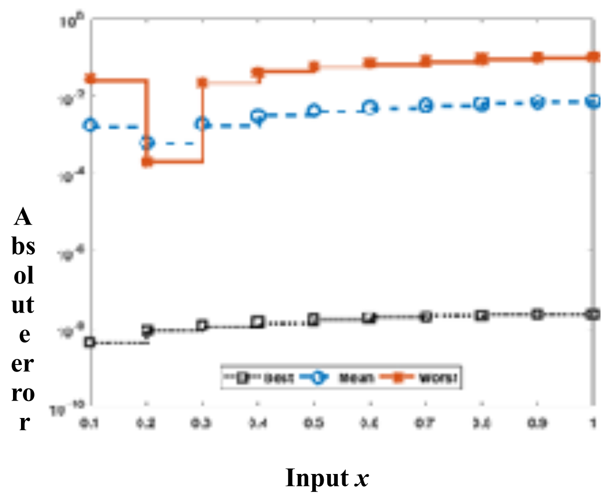

(b) Results of NS-FLE equation Case 2

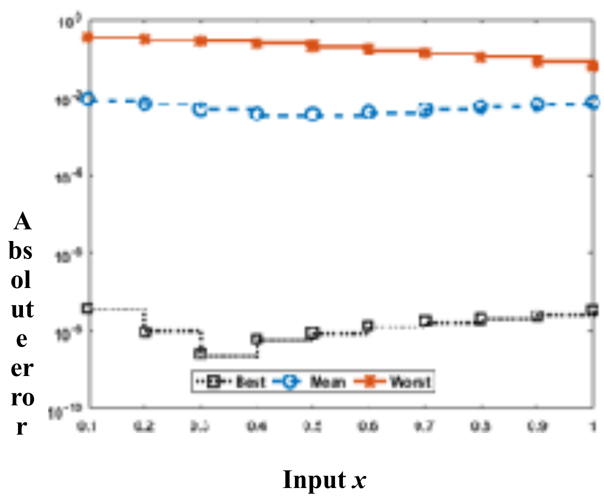

(c) Results of NS-FLE equation Case 3

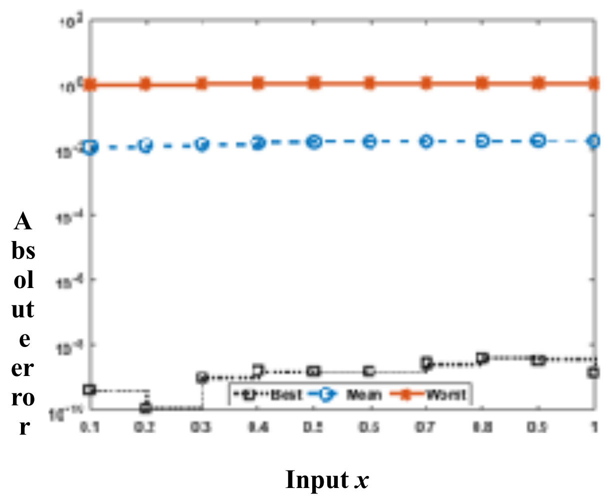

(d) Results of NS-FLE equation Case 4

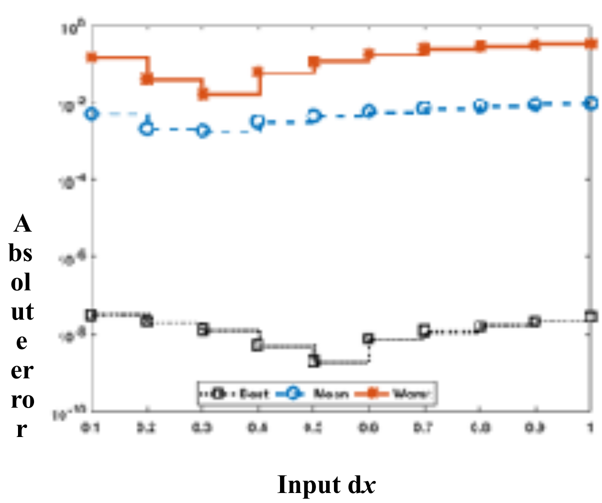

(e) Results of NS-FLE equation Case 5

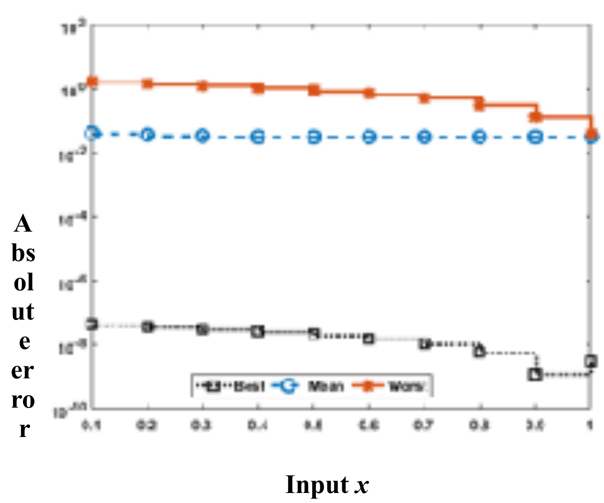

(f) Results of NS-FLE equation Case 4

Figure 5: Statistical operators based comparison through magnitude of AE for all six cases of NS-FLE system

Table 5: Comparison on different statistical metrics for FMW-ANN-GAAS results for cases 1 and 2 of NS-FLE system

x	Case 1				Case 2			
	Min	**Max**	**Median**	**SIR**	**Min**	**Max**	**Med**	**SIR**
0.	8.187E-09	3.428E-02	1.892E-04	6.859E-04	3.332E-09	2.719E-02	1.299E-04	6.724E-04
0.	1.161E-08	4.095E-02	2.455E-04	8.612E-04	6.946E-10	1.174E-02	1.306E-05	6.821E-05
0.	6.429E-09	4.782E-02	2.808E-04	1.111E-03	9.438E-10	2.515E-02	1.248E-04	5.564E-04
0.	3.012E-09	5.554E-02	3.653E-04	1.348E-03	9.053E-09	4.364E-02	2.301E-04	1.004E-03
0.	4.714E-09	5.690E-02	3.834E-04	1.461E-03	1.706E-08	5.699E-02	2.969E-04	1.302E-03
0.	7.569E-09	5.390E-02	3.644E-04	1.390E-03	1.944E-08	6.840E-02	3.461E-04	1.548E-03
0.	6.328E-09	5.397E-02	3.646E-04	1.400E-03	2.107E-08	7.844E-02	3.974E-04	1.718E-03
0.	1.038E-09	5.888E-02	4.019E-04	1.469E-03	2.240E-08	8.904E-02	4.579E-04	1.823E-03
0.	1.649E-09	5.999E-02	4.157E-04	1.520E-03	2.348E-08	9.854E-02	5.088E-04	1.983E-03
1.	1.777E-09	5.339E-02	3.712E-04	1.437E-03	2.429E-08	1.046E-01	5.337E-04	2.266E-03

Table 6: Comparison on different statistical metrics for FMW-ANN-GAAS results for cases 3 and 4 of NS-FLE system

x	Case 3				Case 4			
	Min	**Max**	**Median**	**SIR**	**Min**	**Max**	**Med**	**SIR**
0.	1.611E-08	3.357E-01	1.802E-04	8.486E-04	4.287E-10	1.003E+00	2.076E-04	4.345E-04
0.	1.001E-08	3.035E-01	1.209E-04	6.406E-04	1.200E-10	1.049E+00	2.718E-04	5.604E-04
0.	2.546E-09	2.755E-01	4.835E-05	2.403E-04	1.038E-09	1.063E+00	3.290E-04	6.130E-04
0.	3.245E-09	2.430E-01	4.773E-05	1.977E-04	1.703E-09	1.091E+00	3.658E-04	8.077E-04
0.	9.127E-09	2.043E-01	1.054E-04	4.056E-04	1.529E-09	1.106E+00	3.964E-04	9.960E-04
0.	1.350E-08	1.648E-01	1.238E-04	5.506E-04	1.574E-09	1.100E+00	4.024E-04	1.107E-03
0.	1.789E-08	1.314E-01	1.500E-04	6.515E-04	2.741E-09	1.094E+00	4.107E-04	1.068E-03
0.	2.111E-08	1.322E-01	1.972E-04	7.530E-04	4.198E-09	1.098E+00	4.256E-04	9.845E-04
0.	2.552E-08	1.568E-01	2.446E-04	8.626E-04	3.661E-09	1.093E+00	4.492E-04	1.084E-03
1.	3.409E-08	1.816E-01	2.298E-04	9.549E-04	1.477E-09	1.062E+00	4.522E-04	1.240E-03

Table 7: Comparison on different statistical metrics for FMW-ANN-GAAS results for cases 5 and 6 of NS-FLE system

x	Case 5				Case 6			
	Min	**Max**	**Median**	**SIR**	**Min**	**Max**	**Med**	**SIR**
0.	3.119E-08	1.473E-01	5.108E-04	1.279E-03	4.315E-08	1.673E+00	8.469E-04	3.366E-03
0.	2.039E-08	4.150E-02	1.147E-04	4.117E-04	3.701E-08	1.453E+00	6.651E-04	2.433E-03
0.	9.803E-09	3.636E-02	2.151E-04	6.737E-04	3.127E-08	1.259E+00	3.956E-04	1.573E-03
0.	4.966E-09	6.164E-02	4.865E-04	1.086E-03	1.364E-08	1.075E+00	6.775E-05	5.810E-04
0.	1.956E-09	1.143E-01	6.772E-04	1.144E-03	4.839E-09	8.914E-01	2.936E-04	1.502E-03

0.	7.555E-09	1.760E-01	7.856E-04	1.436E-03	1.563E-08	7.030E-01	4.919E-04	2.144E-03
0.	1.199E-08	2.373E-01	9.630E-04	1.713E-03	1.070E-08	6.616E-01	7.269E-04	3.076E-03
0.	1.623E-08	2.851E-01	1.104E-03	2.011E-03	5.795E-09	7.684E-01	8.869E-04	4.037E-03
0.	2.116E-08	3.131E-01	1.247E-03	2.276E-03	1.184E-09	8.719E-01	1.087E-03	4.880E-03
1.	2.620E-08	3.327E-01	1.375E-03	2.400E-03	3.110E-09	9.672E-01	1.266E-03	5.607E-03

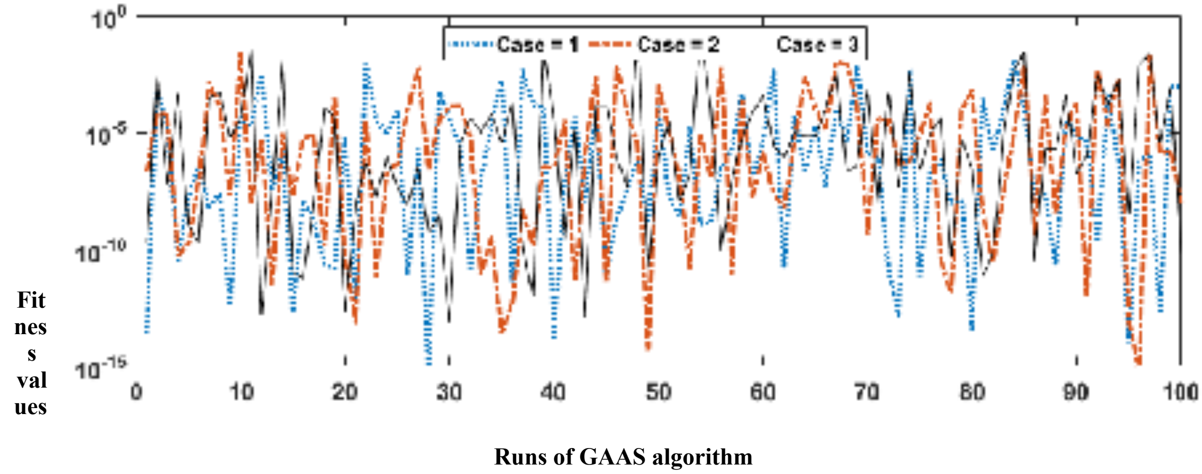

(a) Fitness analysis for Cases 1 to 3 of NS-FLE equation

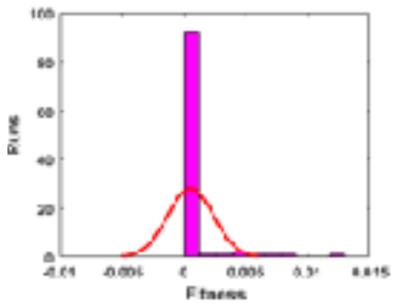

(c): Case 1 histogram

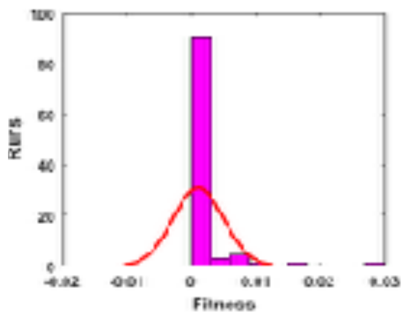

(d): Case 2 histogram

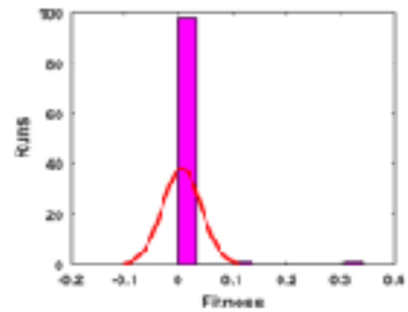

(e): Case 3 histogram

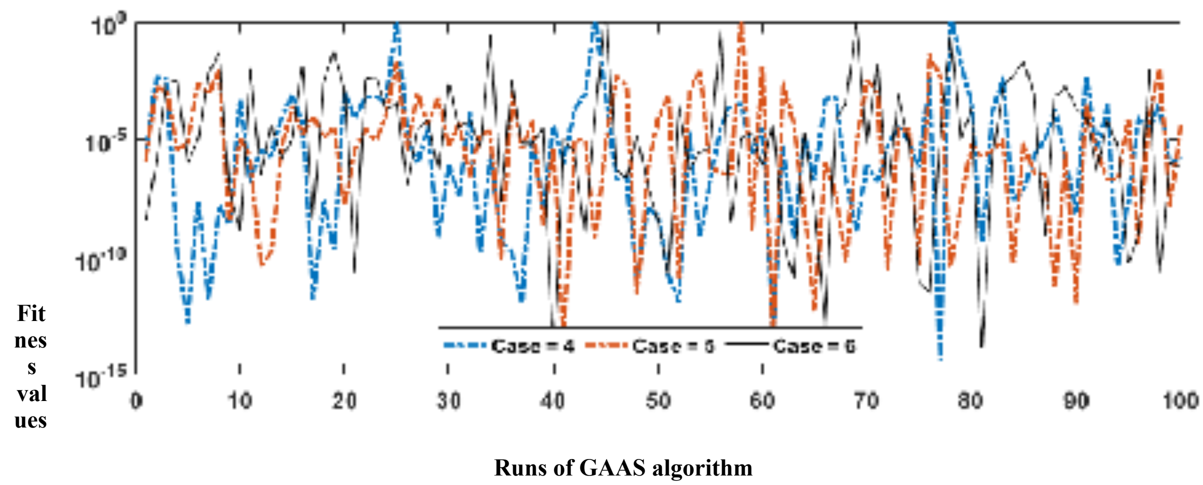

(b) Fitness analysis for Cases 4 to 6 of NS-FLE equation

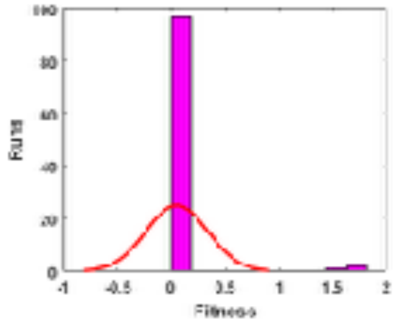

(f): Case 4 histogram

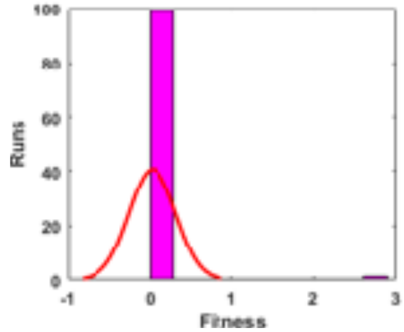

(g): Case 5 histogram

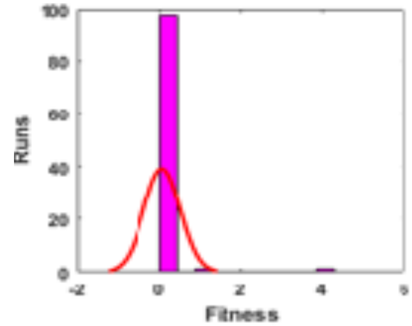

(h): Case 6 histogram

Figure 6: Comparison of results through fitness gauge of GAAS method for all six cases of NS-FLE system

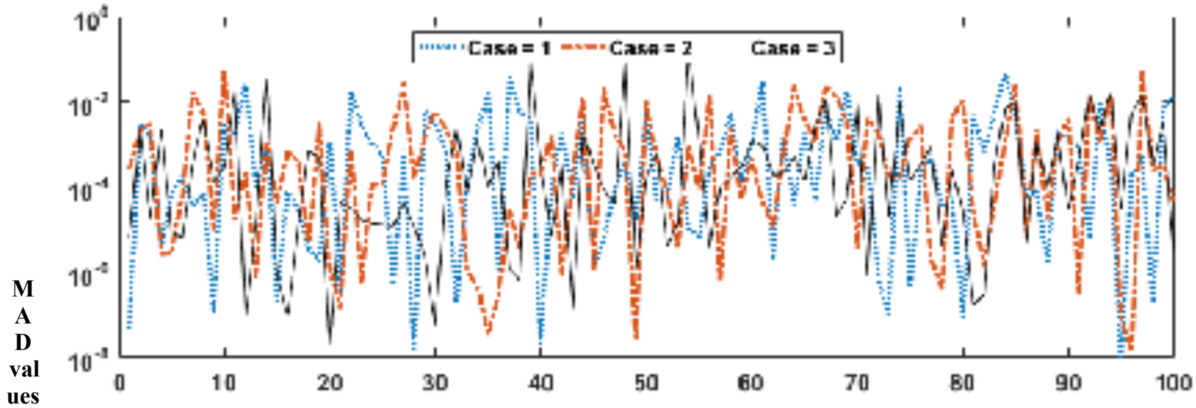

Runs of GAAS algorithm

(a) MAD analysis for Cases 1 to 3 of NS-FLE equation

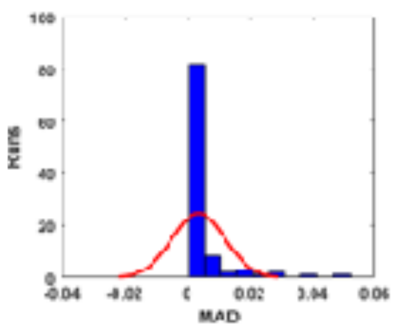

(c): Case 1 histogram

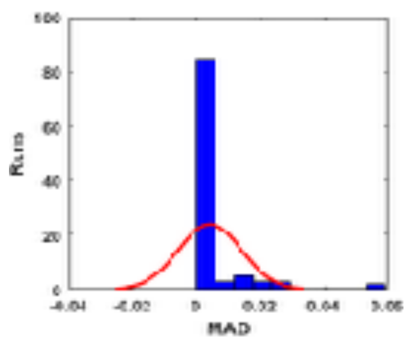

(d): Case 2 histogram

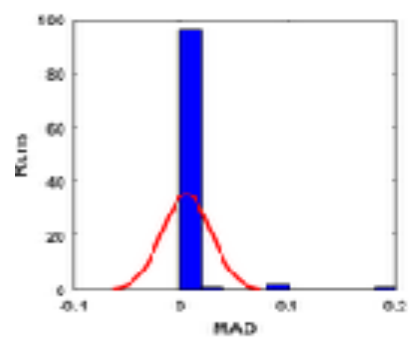

(e): Case 3 histogram

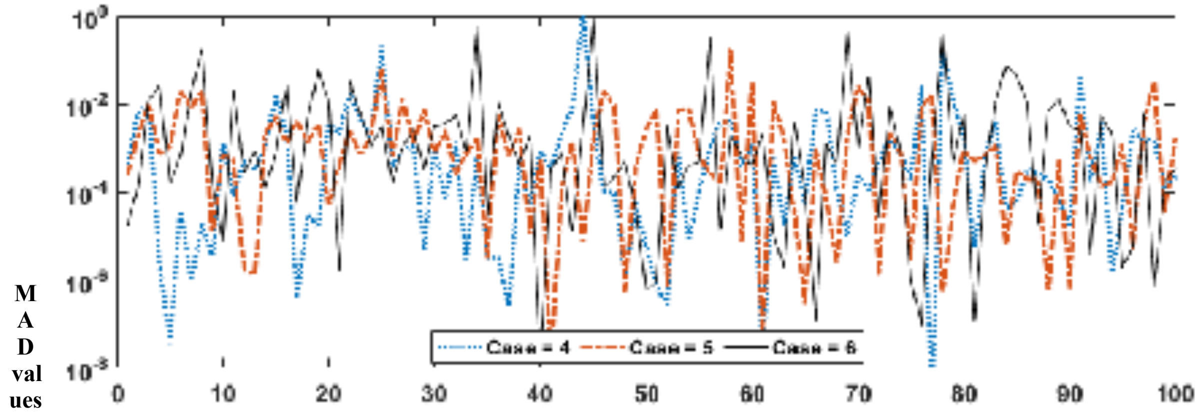

Runs of GAAS algorithm

(b) MAD analysis for Cases 4 to 6 of NS-FLE equation

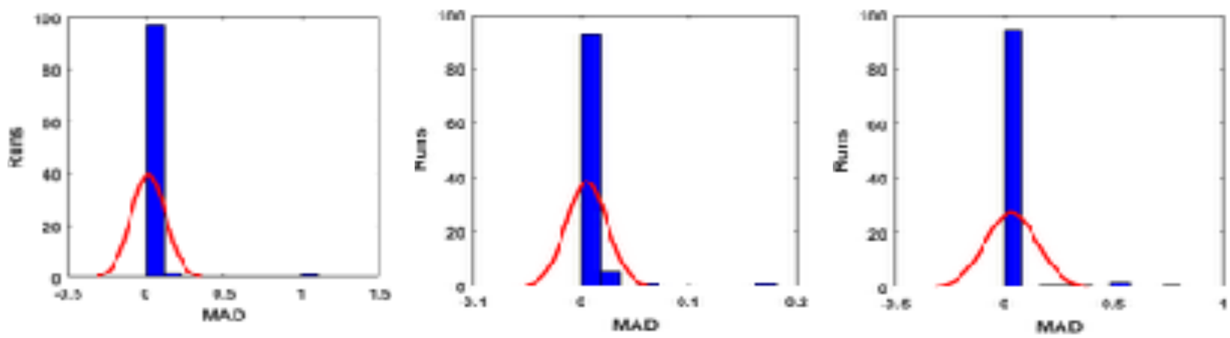

(f): Case 4 histogram (g): Case 5 histogram (h): Case 6 histogram

Figure 7: Comparison of results through MAD gauge of GAAS method for all six cases of NS-FLE system

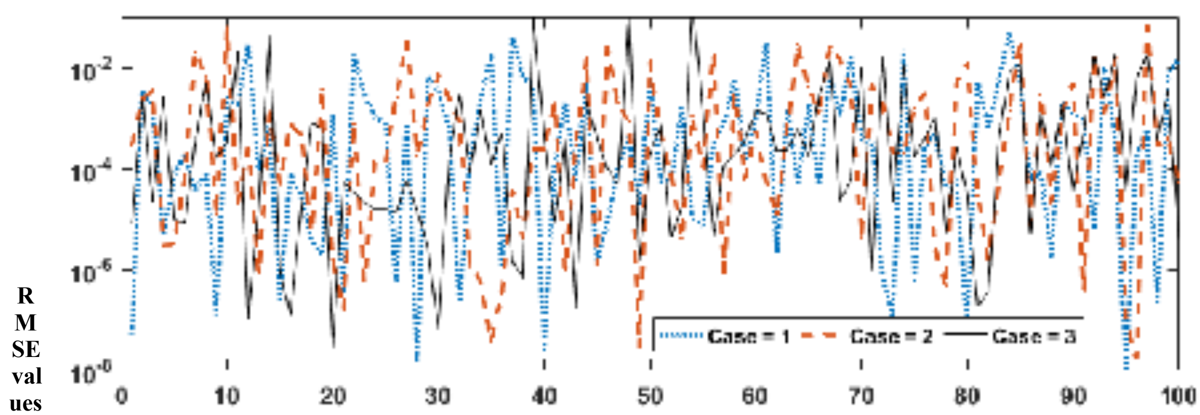

Runs of GAAS algorithm

(a) RMSE analysis for Cases 1 to 3 of NS-FLE equation

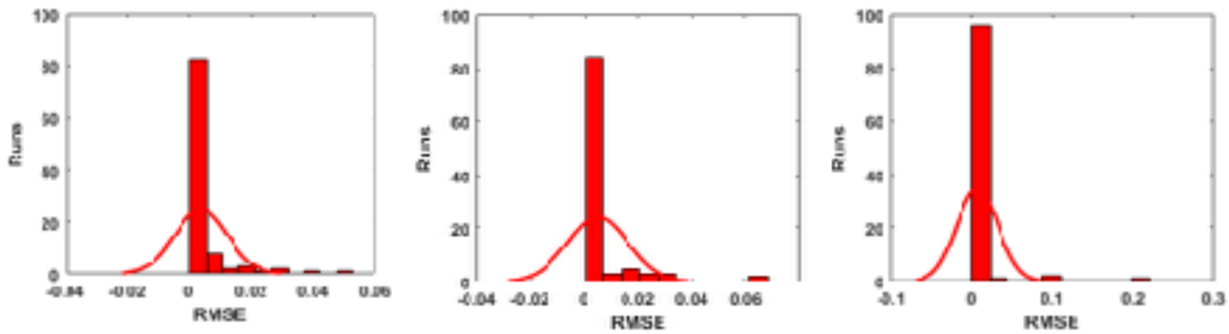

(c): Case 1 histogram (d): Case 2 histogram (e): Case 3 histogram

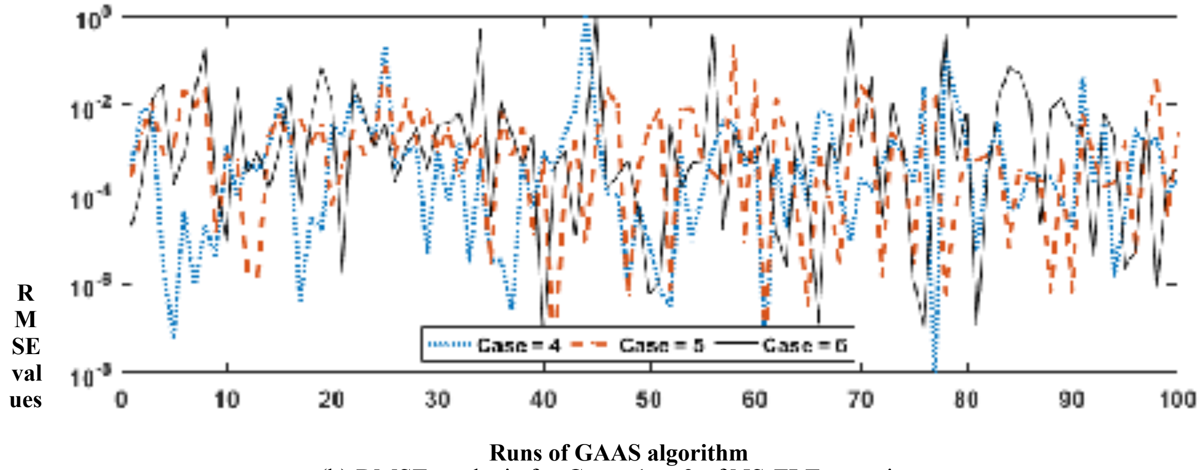

(b) RMSE analysis for Cases 1 to 3 of NS-FLE equation

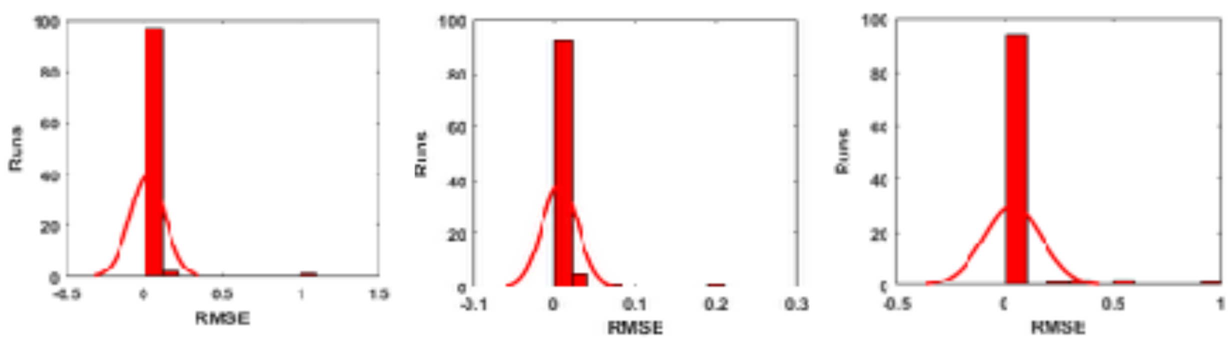

(f): Case 4 histogram (g): Case 5 histogram (h): Case 6 histogram

Figure 8: Comparison of results through RMSE gauge of GAAS method for all six cases of NS-FLE system

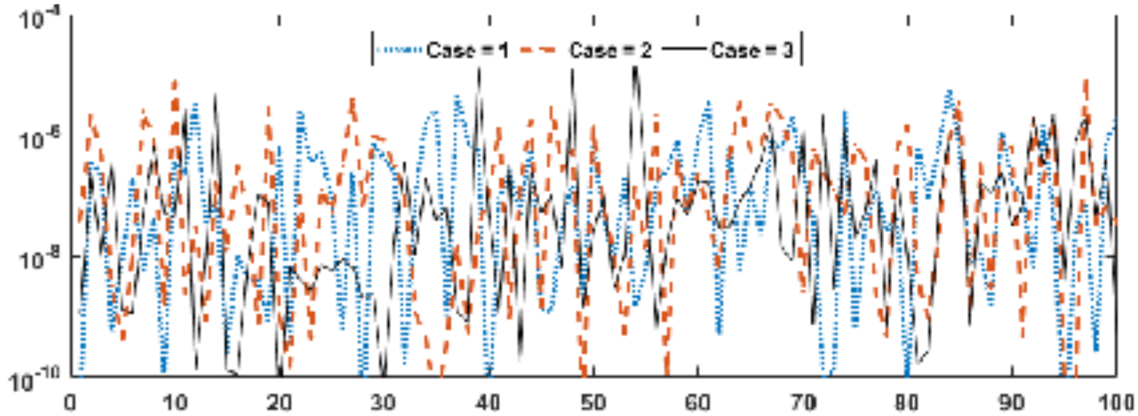

TI
C
val
ues

Runs of GAAS algorithm

(a) Fitness analysis for Cases 1 to 3 of NS-FLE equation

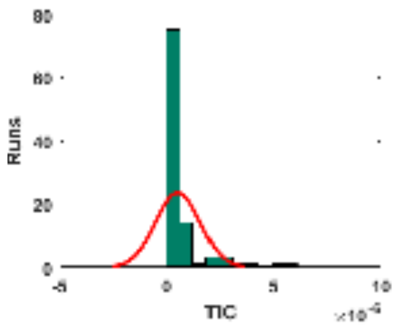

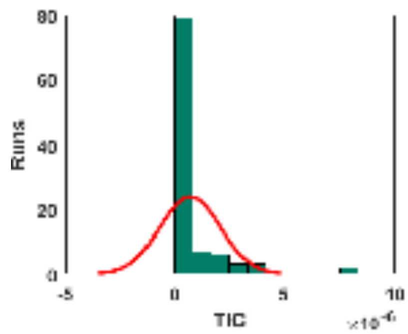

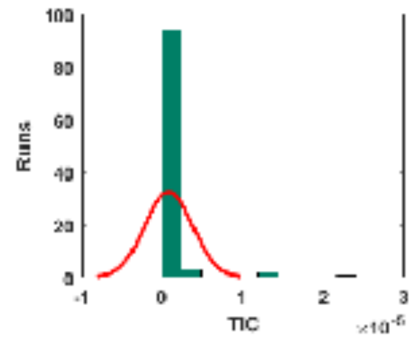

(c): Case 1 histogram (d): Case 2 histogram (e): Case 3 histogram

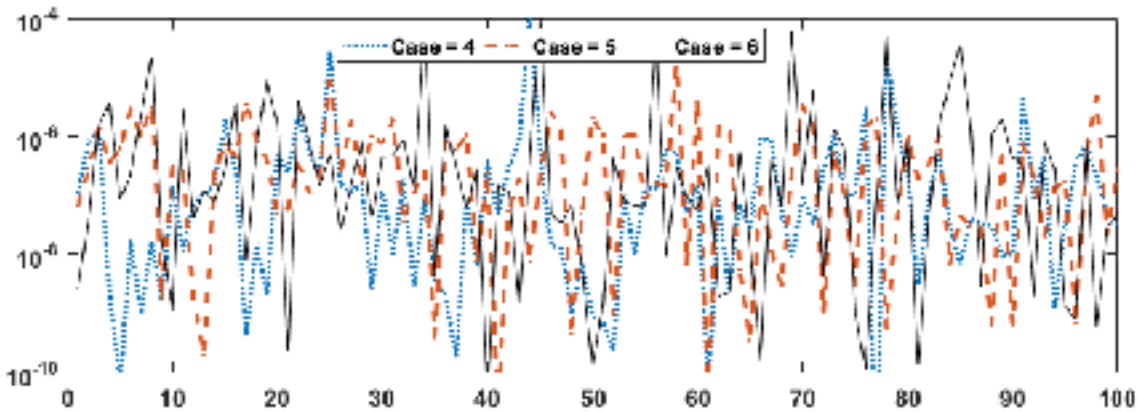

TI
C
val
ues

Runs of GAAS algorithm

(b) TIC analysis for Cases 1 to 3 of NS-FLE equation

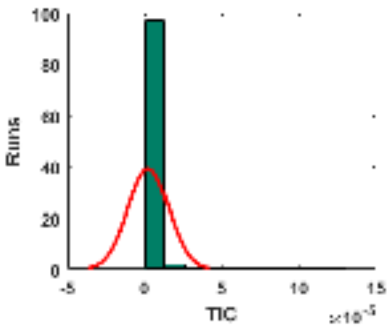

(f): Case 4 histogram

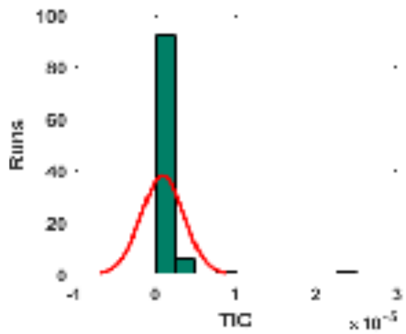

(g): Case 5 histogram

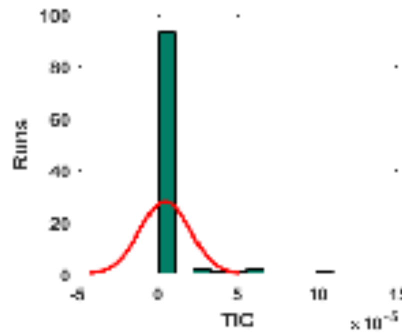

(h): Case 6 histogram

Figure 9: Comparison of results through TIC gauge of GAAS method for all six cases of NS-FLE system

To measure the convergence statistics of proposed FMW-ANN-GAAS scheme, the analysis on the basis of all four performance measures are tabulated in Table 8 for all six cases of NS-FLE system. It is clear, that most of runs obtained the levels ‘FIT ≤ 10^{-03}’, ‘MAD ≤ 10^{-03}’, ‘RMSE ≤ 10^{-04}’ and ‘TIC ≤ 10^{-07}’, while, the reasonable independent trails of FMW-ANN-GA can achieved relatively stiffer levels. Although, for higher precision levels, comparatively number of runs decreased considerably of the present FMW-ANN-GAAS scheme to fulfil the conditions. The convergence analysis of FMW-ANN-GAAS is further conducted on global performance operators based on G-FIT, G-MAD, G-RMSE and G-TIC and these results for 100 runs are tabulated in Table 9. The G-FIT, G-MAD, G-RMSE and G-TIC values lie around 10^{-02} to 10^{-04}, 10^{-02} to 10^{-03}, 10^{-02} to 10^{-03} and 10^{-06} to 10^{-07}, respectively, together with small standard deviation (SD) values. The close to optimal values of these global indices further validate the precision of the presented FMW-ANN-GAAS scheme.

Table 8: Convergence analysis for cases (1-6) of fractional Lane-Emden model

Case	FIT≤			MAD ≤			RMSE≤			TIC ≤		
	10^{-03}	10^{-04}	10^{-05}	10^{-03}	10^{-04}	10^{-05}	10^{-04}	10^{-05}	10^{-06}	10^{-06}	10^{-07}	10^{-08}
1	96	88	76	81	55	31	55	31	21	99	46	26
2	92	85	70	83	54	35	53	33	23	98	43	29
3	92	84	69	85	66	41	65	39	16	97	53	27
4	97	85	71	85	53	34	51	34	21	98	40	25
5	94	78	67	76	52	30	51	29	18	96	41	25
6	86	72	58	76	47	25	46	23	13	93	37	15

Table 9: Global performance for cases (1-6) of Lane-Emden model

Case	GFIT		GMAD		GRMSE		GTIC	
	Mag	SD	Mag	SD	Mag	SD	Mag	SD
1	5.29E-04	1.85E-03	3.60E-03	8.42E-03	3.66E-03	8.54E-03	5.16E-07	1.03E-06

2	1.11E-03	3.89E-03	4.24E-03	9.89E-03	4.81E-03	1.13E-02	6.89E-07	1.38E-06
3	6.06E-03	3.56E-02	5.61E-03	2.26E-02	6.39E-03	2.55E-02	7.75E-07	2.96E-06
4	5.07E-02	2.87E-01	1.66E-02	1.10E-01	1.70E-02	1.11E-01	2.09E-06	1.33E-05
5	2.98E-02	2.84E-01	5.57E-03	1.87E-02	6.43E-03	2.21E-02	9.31E-07	2.64E-06
6	6.48E-02	4.39E-01	3.24E-02	1.18E-01	3.60E-02	1.34E-01	4.51E-06	1.57E-05

The computational cost of the presented FMW-ANN-GAAS algorithm are examined through completed iterations/cycles, average time of parameter adaptation and executed function counts during the process of find the decision variable of the networks. Complexity analysis for each case of NS-FLE model are determined and the outcomes are listed in Table 10. One may observe that the average generations/iterations, time and evaluations of functions are around 212.95, 537.74 and 48888.28, for all six cases of NS-FLE system, respectively. These values are given to compare the efficiency of the proposed FMW-ANN-GAAS scheme.

Table 10: Complexity analysis for cases (1-6) of Lane-Emden model

Case	Generation/Iteration		Time of execution		Function Counts	
	Mean	**SD**	**Mean**	**SD**	**Mean**	**SD**
1	170.6794	155.1256	492.01	279.9201	46055.45	19278.42
2	174.8195	162.6908	498.3	280.3729	46249.79	18818.14
3	189.8958	159.454	570.01	262.5481	50665.97	17410.45
4	188.4489	161.5488	533.53	270.1939	48694.47	18269.01
5	325.7306	1421.96	503.62	274.4711	46678.66	18511.97
6	228.1427	181.5433	628.94	223.0223	54985.35	15166.35

5. Conclusions

A new stochastic computational solver FMW-ANN-GASA based on fractional Mayer wavelet artificial neural network optimized with integrated strength of genetic algorithm aid with active-set method is presented for reliable and effective numerical treatment for nonlinear singular fractional Lane-Emden differential equation. The proposed FMW-ANN-GASA methodology is viably implemented on fractional Lane-Emden system for six different scenarios to prove its accuracy, convergence, stability and robustness. Comparison of the proposed numerical solutions of FMW-ANN-GASA with exact solutions shows the matching of order 7 to 10 decimal places of accuracy which verify its correctness and efficacy. Statistical measures of the present results indicate that more than 75% runs of the algorithm give precise results consistently. Consequently, the present technique is not only effective but one can implement easily too. The proposed FMW-ANN-GAAS is a fast convergent procedure that can implemented to solve the linear/ nonlinear, singular/nonsingular systems governed with differential equation.

In future, one may exploit the FMW-ANN-GASA scheme for solution of fractional order systems represented with nonlinear Riccati equation, Baglay-Torvik equation, Van-der Pol system and Painleve eqautions.

Non conflict Statement

The authors declare that there is no conflict of interest between them and the journal. This paper has been partially supported by Ministerio de Ciencia, Innovación y Univesidades grant number PGC2018-097198-B-100 and Fundación Séneca grant number 20783/PI/18.

References

[1] Diethelm, K., Ford, N. J. (2002). Analysis of fractional differential equations. *Journal of Mathematical Analysis and Applications*, *265*(2), 229-248.

[2] Yu, F. (2009). Integrable coupling system of fractional soliton equation hierarchy. Physics Letters A, 373(41), 3730-3733.

[3] Momani, S., Ibrahim, R. W. (2008). On a fractional integral equation of periodic functions involving Weyl–Riesz operator in Banach algebras. Journal of Mathematical Analysis and Applications, 339(2), 1210-1219.

[4] Ibrahim, R. W., Momani, S. (2007). On the existence and uniqueness of solutions of a class of fractional differential equations. Journal of Mathematical Analysis and Applications, 334(1), 1-10.

[5] Bonilla, B., Rivero, M., Trujillo, J. J. (2007). On systems of linear fractional differential equations with constant coefficients. Applied Mathematics and Computation, 187(1), 68-78.

[6] I. Podlubny, (1999). Fractional Differential Equations," Acade- mic Press, London

[7] Diethelm, K., Freed, A. D. (1999). On the solution of nonlinear fractional-order differential equations used in the modeling of viscoplasticity. In Scientific Computing in Chemical Engineering II (pp. 217-224). Springer, Berlin, Heidelberg.

[8] Podlubny, I., Dorcak, L., Kostial, I. (1997, December). On fractional derivatives, fractional-order dynamic systems and PI/sup/spl lambda//D/sup/spl mu//-controllers. In Proceedings of the 36th IEEE Conference on Decision and Control (Vol. 5, pp. 4985-4990). IEEE.

[9] Agrawal, O.P., 2004. Application of fractional derivatives in thermal analysis of disk brakes. Nonlinear Dynamics, 38(1-4), pp.191-206.

[10] Torvik, P. J., Bagley, R. L. (1984). On the appearance of the fractional derivative in the behavior of real materials. Journal of Applied Mechanics, 51(2), 294-298.

[11] Momani, S., Odibat, Z. (2006). Analytical approach to linear fractional partial differential equations arising in fluid mechanics. Physics Letters A, 355(4-5), 271-279.

[12] Hilfer, R. (2002). Experimental evidence for fractional time evolution in glass forming materials. Chemical Physics, 284(1-2), 399-408.

[13] Engheia, N. (1997). On the role of fractional calculus in electromagnetic theory. IEEE Antennas and Propagation Magazine, 39(4), 35-46.

[14] Makris, N., Constantinou, M. C. (1991). Fractional-derivative Maxwell model for viscous dampers. Journal of Structural Engineering, 117(9), 2708-2724.

[15] Jiang, H., Cheng, Y., Yuan, L., An, F., and Jin, K. (2013). A fractal theory based fractional diffusion model used for the fast desorption process of methane in coal. Chaos: An Interdisciplinary Journal of Nonlinear Science, 23(3), 033111.

[16] Burgos, C., Cortés, J. C., Villafuerte, L., and Villanueva, R. J. (2017). Mean square calculus and random linear fractional differential equations: Theory and applications. Applied Mathematics and Nonlinear Sciences, 2(2), 317-328.

[17] Brzeziński, D. W. (2018). Review of numerical methods for NumILPT with computational accuracy assessment for fractional calculus. Applied Mathematics and Nonlinear Sciences, 3(2), 487-502.

[18] Yıldırım, A., Öziş, T. (2007). Solutions of singular IVPs of Lane–Emden type by homotopy perturbation method. Physics Letters A, 369(1-2), 70-76.

[19] Parand, K., Pirkhedri, A. (2010). Sinc-collocation method for solving astrophysics equations. New Astronomy, 15(6), 533-537.

[20] Yıldırım, A., Öziş, T. (2009). Solutions of singular IVPs of Lane–Emden type by the variational iteration method. Nonlinear Analysis: Theory, Methods & Applications, 70(6), 2480-2484.

[21] Parand, K., Dehghan, M., Rezaei, A. R., & Ghaderi, S. M. (2010). An approximation algorithm for the solution of the nonlinear Lane–Emden type equations arising in astrophysics using Hermite functions collocation method. Computer Physics Communications, 181(6), 1096-1108.

[22] Doha, E. H., Abd-Elhameed, W. M., & Youssri, Y. H. (2013). Second kind Chebyshev operational matrix algorithm for solving differential equations of Lane–Emden type. New Astronomy, 23, 113-117.

[23] Yousefi, S. A. (2006). Legendre wavelets method for solving differential equations of Lane–Emden type. Applied Mathematics and Computation, 181(2), 1417-1422.

[24] Parand, K., Nikarya, M., & Rad, J. A. (2013). Solving non-linear Lane–Emden type equations using Bessel orthogonal functions collocation method. Celestial Mechanics and Dynamical Astronomy, 116(1), 97-107.

[25] Mechee, M. S., Senu, N. (2012). Numerical study of fractional differential equations of Lane-Emden type by method of collocation. Applied Mathematics, 3(08), 851.

[26] Masood, Z., et al., 2017. Design of Mexican Hat Wavelet neural networks for solving Bratu type nonlinear systems. *Neurocomputing*, *221*, pp.1-14.

[27] Raja, M.A.Z., Niazi, S.A. and Butt, S.A., 2017. An intelligent computing technique to analyze the vibrational dynamics of rotating electrical machine. *Neurocomputing*, *219*, pp.280-299.

[28] Berg, J. and Nyström, K., 2018. A unified deep artificial neural network approach to partial differential equations in complex geometries. *Neurocomputing*, *317*, pp.28-41.

[29 Pakdaman, M., Ahmadian, A., Effati, S., Salahshour, S. and Baleanu, D., 2017. Solving differential equations of fractional order using an optimization technique based on training artificial neural network. *Applied Mathematics and Computation*, *293*, pp.81-95.

[30] Jafarian, A., Nia, S.M., Golmankhaneh, A.K. and Baleanu, D., 2018. On artificial neural networks approach with new cost functions. *Applied Mathematics and Computation*, *339*, pp.546-555.

[31] Schaff, J. C., Gao, F., Li, Y., Novak, I. L., & Slepchenko, B. M. (2016). Numerical approach to spatial deterministic-stochastic models arising in cell biology. PLoS computational biology, 12(12), e1005236.

[32] Umar, M., et al., (2019). Intelligent computing for numerical treatment of nonlinear prey–predator models. Applied Soft Computing, 80, 506-524.

[33] Ahmad, I., et al., (2019) Novel applications of intelligent computing paradigms for the analysis of nonlinear reactive transport model of the fluid in soft tissues and microvessels. *Neural Computing and Applications*, In press, https://doi.org/10.1007/s00521-019-04203-y.

[34] Raja, M. A. Z., Shah, F. H., Tariq, M., and Ahmad, I. (2018). Design of artificial neural network models optimized with sequential quadratic programming to study the dynamics of nonlinear Troesch's problem arising in plasma physics. Neural Computing and Applications, 29(6), 83-109.

[35] Sabir, Z., et al., (2018). Neuro-heuristics for nonlinear singular Thomas-Fermi systems. Applied Soft Computing, 65, 152-169.

[36] Raja, M. A. Z., Mehmood, J., Sabir, Z., Nasab, A. K., and Manzar, M. A. (2019). Numerical solution of doubly singular nonlinear systems using neural networks-based integrated intelligent computing. Neural Computing and Applications, 31(3), 793-812.

[37] Mehmood, A., et al., 2019. Integrated intelligent computing paradigm for the dynamics of micropolar fluid flow with heat transfer in a permeable walled channel. *Applied Soft Computing*, *79*, pp.139-162.

[38] Mehmood, A., et al., 2018. Intelligent computing to analyze the dynamics of magnetohydrodynamic flow over stretchable rotating disk model. *Applied Soft Computing*, *67*, pp.8-28.

[39] Raja, M. A. Z., Shah, F. H., Alaidarous, E. S., & Syam, M. I. (2017). Design of bio-inspired heuristic technique integrated with interior-point algorithm to analyze the dynamics of heartbeat model. Applied Soft Computing, 52, 605-629.

[40] He, W., Chen, Y., and Yin, Z. (2016). Adaptive neural network control of an uncertain robot with full-state constraints. IEEE transactions on cybernetics, 46(3), 620-629.

[41] Raja, M. A. Z., Umar, M., Sabir, Z., Khan, J. A., and Baleanu, D. (2018). A new stochastic computing paradigm for the dynamics of nonlinear singular heat conduction model of the human head. The European Physical Journal Plus, 133(9), 364.

[42] Pelletier, F., Masson, C., and Tahan, A. (2016). Wind turbine power curve modelling using artificial neural network. Renewable Energy, 89, 207-214.

[43] Zameer, A., et al., 2017. Intelligent and robust prediction of short term wind power using genetic programming based ensemble of neural networks. *Energy conversion and management*, *134*, pp.361-372.

[44] Lodhi, S., Manzar, M.A. and Raja, M.A.Z., 2019. Fractional neural network models for nonlinear Riccati systems. *Neural Computing and Applications*, *31*(1), pp.359-378.

[45] Raja, M.A.Z., Samar, R., Manzar, M.A. and Shah, S.M., 2017. Design of unsupervised fractional neural network model optimized with interior point algorithm for solving Bagley–Torvik equation. *Mathematics and Computers in Simulation*, *132*, pp.139-158.

[46] Artar, M. and Daloğlu, A.T., 2018. Optimum weight design of steel space frames with semi-rigid connections using harmony search and genetic algorithms. *Neural Computing and Applications*, *29*(11), pp.1089-1100.

[47] Flórez, C.A.C., Rosário, J.M. and Amaya, D., 2018. Control structure for a car-like robot using artificial neural networks and genetic algorithms. *Neural Computing and Applications*, pp.1-14.

[48] Adánez, J.M., Al-Hadithi, B.M. and Jiménez, A., 2019. Multidimensional membership functions in T–S fuzzy models for modelling and identification of nonlinear multivariable systems using genetic algorithms. *Applied Soft Computing*, *75*, pp.607-615.

[49] de Almeida, B.J., Neves, R.F. and Horta, N., 2018. Combining Support Vector Machine with Genetic Algorithms to optimize investments in Forex markets with high leverage. *Applied Soft Computing*, *64*, pp.596-613.

[50] Peker, M., 2018. A fully customizable hardware implementation for general purpose genetic algorithms. *Applied Soft Computing*, *62*, pp.1066-1076.

[51] Fernández, J.R., López-Campos, J.A., Segade, A. and Vilán, J.A., 2018. A genetic algorithm for the characterization of hyperelastic materials. *Applied Mathematics and Computation*, *329*, pp.239-250.

[52] Bonakdari, H., Khozani, Z.S., Zaji, A.H. and Asadpour, N., 2018. Evaluating the apparent shear stress in prismatic compound channels using the Genetic Algorithm based on Multi-Layer Perceptron: A comparative study. *Applied Mathematics and Computation*, *338*, pp. 400-411.

[53] Tian, D., Deng, J., Vinod, G., Santhosh, T.V. and Tawfik, H., 2018. A constraint-based genetic algorithm for optimizing neural network architectures for detection of loss of coolant accidents of nuclear power plants. *Neurocomputing*, *322*, pp.102-119.

[54] Pei, X., Zhou, Y. and Wang, N., 2019. A Gaussian process regression based on variable parameters fuzzy dominance genetic algorithm for B-TFPMM torque estimation. *Neurocomputing*, *335*, pp.153-169.

[55] Zhong, S., Xie, X., Lin, L. and Wang, F., 2017. Genetic algorithm optimized double-reservoir echo state network for multi-regime time series prediction. *Neurocomputing*, *238*, pp.191-204.

[56] Raja, M.A.Z., Mehmood, A., ur Rehman, A., Khan, A. and Zameer, A., 2018. Bio-inspired computational heuristics for Sisko fluid flow and heat transfer models. *Applied Soft Computing*, *71*, pp.622-648.

[57] Zhao, M. H., Ding, X. F., Shi, Z. H., Yao, Q. Z., Yuan, Y. Q. and Mo, R. Y. (2016). An efficient active set method for optimization extreme learning machines. Neurocomputing, 174, 187-193.

[58] Brás, C.P., Fischer, A., Júdice, J.J., Schönefeld, K. and Seifert, S., 2017. A block active set algorithm with spectral choice line search for the symmetric eigenvalue complementarity problem. *Applied Mathematics and Computation*, *294*, pp.36-48..

[59] Ahmad, I., et al., 2018. Intelligent computing to solve fifth-order boundary value problem arising in induction motor models. *Neural Computing and Applications*, *29*(7), pp. 449-466.
[60] Munir, A., et al., 2019. Intelligent computing approach to analyze the dynamics of wire coating with Oldroyd 8-constant fluid. *Neural Computing and Applications*, *31*(3), pp. 751-775.
[61] Chamakuri, N., & Kunisch, K. (2017). Primal-dual active set strategy for large scale optimization of cardiac defibrillation. Applied Mathematics and Computation, 292, 178-193.